A solid state NMR study of Layered double hydroxides intercalated with para-amino salicylate, a tuberculosis drug

Jensen, Nicholai Daugaard; Bjerring, Morten; Nielsen, Ulla Gro

Published in:
Solid State Nuclear Magnetic Resonance

DOI:
10.1016/j.ssnmr.2016.06.001

Publication date:
2016

Document version
Peer reviewed version

A solid state NMR study of layered double hydroxides intercalated with para-amino salicylate, a tuberculosis drug

Nicholai Daugaard Jensen[1], Morten Bjerring[2], and Ulla Gro Nielsen[1,*]

[1] Department of Physics, Chemistry, and Pharmacy, University of Southern Denmark, Campusvej 55, 5230 Odense M, Denmark

[2] Department of Chemistry and Interdisciplinary Nanoscience Center (iNANO), University of Aarhus, Gustav Wiedsvej 14,8000 Aarhus C, Denmark

*corresponding author: email ugn@sdu.dk phone + 456550 4401

Highlights:

- Incorporation of para-amino salicylate in LDHs was confirmed by solid state NMR
- In depth investigations of the cation- and interlayer in layered double hydroxides
- Amorphous aluminium impurities are only detected by solid state NMR
- The first high-resolution ^{1}H NMR data of a CaAl layered double hydroxide

Abstract:

Para-amino salicylate (PAS), a tubercolosis drug, was intercalated in three different layered double hydroxides (MgAl, ZnAl, and CaAl-LDH) and the samples were studied by multi-nuclear (^{1}H, ^{13}C, and ^{27}Al) solid state NMR (SSNMR) spectroscopy in combination with powder X-ray diffraction (PXRD),

elemental analysis and IR-spectroscopy to gain insight into the bulk and atomic level structure of these LDHs especially with a view to the purity of the LDH-PAS materials and the concentration of impurities. The intercalations of PAS in MgAl-, ZnAl-, and CaAl-LDH's were confirmed by ^{13}C SSNMR and PXRD. Moreover, ^{13}C MAS NMR and infra-red spectroscopy show that PAS did not decompose during synthesis. Large amounts (20-41 %) of amorphous aluminum impurities were detected in the structure using ^{27}Al single pulse and 3QMAS NMR spectra, which in combination with ^{1}H single and double quantum experiments also showed that the M(II):Al ratio was higher than predicted from the bulk metal composition of MgAl-PAS and ZnAl-PAS. Moreover, the first high-resolution ^{1}H SSNMR spectra of a CaAl LDH is reported and assigned using ^{1}H single and double quantum experiments in combination with $^{27}Al\{^{1}H\}$ HETCOR.

Keywords: layered double hydroxides; para-amino salicylic acid; para-amino salicylate solid state NMR; ^{27}Al; ^{1}H; local environment; nanocomposite

Graphical Abstract:

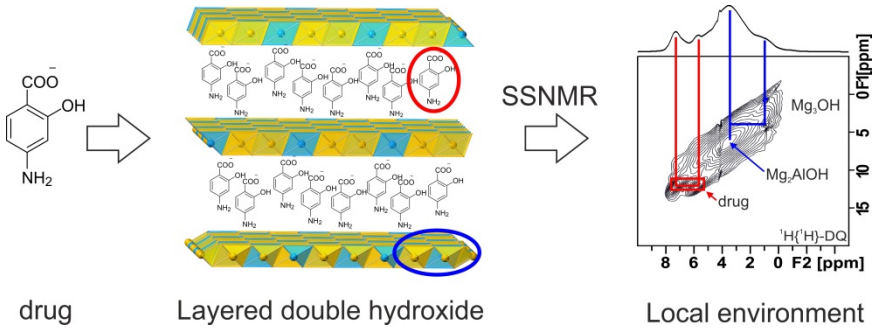

1. Introduction

Layered double hydroxides (LDHs) are a versatile class of inorganic materials which find wide-spread application in many areas ranging from catalysis, energy storage and conversion to environmental remediation and drug delivery[1-5]. They have a general composition of $[M(II)_{1-x}M(III)_x(OH)_2A_y\ nH_2O]$ where M(II) and M(III) are a wide range of cation such as Mg(II), Ca(II), Zn(II), Al(III), and Fe(III), and A is an anion needed for charge balance, c.f. Fig. 1[4, 6]. The LDH structure consists of positively charged cation layers obtained by substitution of trivalent cations ($1/6 < x < 1/3$) for divalent, with a variable number of water molecules and an appropriate number of anions intercalated in the interlayer. The anions can be replaced by simple anion-exchange, which has great potential for use in drug delivery, where drugs intercalated in LDHs may be released in a controlled fashion. A large number of active drug molecules exist as anions including many non-steroidal anti-inflammatory drugs (NSAIDS) such as ibuprofen, naproxene, and salicylic acid[7, 8]. Thus, intercalation of these in an LDH may potentially help overcome bioavailability and biosolubility issues of such drugs as well as extend the pharmaceutic effect of the drug by the LDH acting as a retard formulation[9]. A slow release of the drug is obtained by intercalation of these in an LDH matrix, which is slowly dissolved in the body[1, 9]. It is essential to fully understand the intercalation of drug molecule in LDHs and characterize the LDH-drug prior to use. For example, the presence of impurities can lead to unwanted side effects and to degradation of the drug during storage will render it less efficient. However, characterization of LDHs especially with large anions such as organic drug molecules is challenging due to the presence of stacking faults, which makes a precise determination of the structure by diffraction techniques extremely difficult[6]. Moreover, the presence of amorphous impurities in combination with the strict regulations on the purity of pharmaceutical products represent a problem for the use of LDHs in drug delivery, as these impurities are difficult to identify and quantify. To fully understand the composition

of LDH, bulk characterization techniques such as powered X-ray diffraction (PXRD), elemental analysis and microscopy must be combined with probes of the local environment such as vibrational spectroscopy, e.g., Raman and Infra-Red (IR) spectroscopy, as well as solid state NMR spectroscopy (SSNMR)[10]. SSNMR especially has provided detailed insight into both the local structure of LDHs revealing cation ordering in the cation layer[10-14], the dynamics of organic and inorganic anions in the interlayer[15-17]. Moreover, SSNMR has only been used in a few studies of drug molecules such as benzoxaboraolates, salicylic acid, ibuprofen, and L-dopa intercalated in LDHs[8, 18-21]. However, these have been mainly focused on characterization of the drug molecule in the LDH matrix. Generally, only simple 1D spectra have been reported, except for a recent multi-nuclear study of benzoxaboraolates in LDHs[18].

Here we present the results of a detailed SSNMR study of three LDHs (MgAl, ZnAl, and CaAl) intercalated with para-amino salicylate, a tuberculosis drug, in combination with elemental analysis, PXRD and infra-red (IR) spectroscopy, which provides information on both the local and bulk properties of the LDH-drug. The objective is to demonstrate the use of advanced SSNMR techniques to obtain structural information and assess the quality of the LDH-drug product with special focus on the identification and quantification of impurities as well as the structural information about the LDH-PAS on the atomic level. ^{1}H single and double quantum (DQ) SSNMR experiments as well as ^{27}Al 3QMAS and ^{27}Al{^{1}H} HETCOR SSNMR experiments were carried out at 950 MHz resulting in a SSNMR spectra of high resolution, which allowed for quantification of the impurities, the intercalation of the drug and the chemical composition of the LDH layer. Moreover, SSNMR data were obtained at moderate magnetic fields (11.7 and 14.1T) and the results were combined with the ultrahigh field data.

2. Experimental

2.1 Synthesis

All chemicals used were purchased from Sigma-Aldrich, had a purity of ≥ 98 % and were used without further purification. All syntheses were done using decarbonated water and in a nitrogen atmosphere to minimize carbonate impurities. Decarbonated water was obtained by bubbling nitrogen through boiling Milli-Q water for 30 min. A Metrohm Titrando 905 was used for addition of the metal salt solutions and to control the pH by addition of 1 M sodium hydroxide (NaOH). Detailed information about the synthesis is given in the supporting information (Table SI-1). Three different M(II)Al LDHs $[M(II)_2Al(OH)_6(PAS)]$ with M = Mg, Zn, and Ca were prepared by direct incorporation of PAS in the LDH using co-precipitation at constant pH, which is a standard method for preparation and gives the least defective LDHs[10]. These samples will be referred to as MgAl-PAS, ZnAl-PAS and CaAl-PAS, respectively. An excess of PAS was suspended in 30 mL of decarbonated water and the pH adjusted to 10, 8.5, and 12 for M(II) = Mg, Zn, and Ca, respectively, by addition of 1 M NaOH. 10 mL of an aqueous solution of the appropriate $M(II)(NO_3)_2 \cdot nH_2O$ salts ($Mg(NO_3)_2 \cdot 6H_2O$, $Zn(NO_3)_2 \cdot 6H_2O$ or $Ca(NO_3)_2 \cdot 4H_2O$) and $Al(NO_3)_2 \cdot 9H_2O$ with a molar ratio of 2:1 and a total cation concentration of 1 M was added at a rate of 0.2 mL/min while the pH was maintained by simultaneous addition of 1 M NaOH. The product was filtered after ageing at 65 ºC for a minimum of 15 h, washed with a 1:1 mixture of decarbonized water and ethanol and subsequently dried at 65º C. A deuterated sample of MgAl-PAS was obtained by chemical exchange: ca 100 mg of sample was suspended in 10 mL of D_2O and stirred for 8 days, followed by filtering and drying in a desiccator.

2.2 Characterization by PXRD and inductively coupled plasma chromatography (ICP)

The PXRD diffractograms were recorded on a Rigaku miniflex 600 using a $CuK_{\alpha,\beta}$ at 40 kV and 15 mA in the 2θ range from 3 to 70º. The PXRD diffractograms were analyzed using X'Pert HighScore Plus 3.0.0. The Ca, Zn, Mg, and Al content were determined using inductively coupled plasma chromatography (ICP) and the resulting Al content (%) is reported in Table 1.

2.3 Fourier Transformed Infrared Spectroscopy (FTIR)

FTIR was measured using a Perkin Elmer 1720 Infrared Fourier Transform Spectrometer. The FTIR spectra were recorded of pellets made of KBr mixed with 1 mg of the sample in a range from 450 to 4000 cm^{-1} (Supporting information, Fig. SI-2 and Table SI-2).

2.4 Solid State NMR spectroscopy

Single pulse ^{27}Al (quantitative) and ^{13}C CP MAS SSNMR spectra were recorded on a Varian INOVA 500 MHz NMR spectrometer (11.7 T) using a 3.2 mm HX MAS probe and 12 - 15 kHz spinning. ^{27}Al 3QMAS NMR spectra were recorded on a Varian INOVA 600 MHz NMR spectrometer (14.1 T) using a 3.2 mm MAS probe using a Z-filter sequence[22] and 15 kHz spinning. Single pulse ^{27}Al and ^{1}H NMR, $^{1}H\{^{27}Al\}$ HETCOR, and ^{1}H double quantum (DQ) MAS NMR spectra were recorded on a Bruker 950 MHz spectrometer (22.3 T) using a 2.5 mm MAS probe and 35 kHz spinning. The $^{1}H\{^{27}Al\}$ HETCOR spectra were recorded using 0.5 ms contact time to probe short ^{27}Al-^{1}H distances, i.e., directly bonded hydroxyl groups. The ^{1}H DQ MAS NMR spectra were recorded using a BABA sequence[23, 24] Chemical shifts are referenced relative to a 1 M $AlCl_3$ solution ($\delta_{iso}(^{27}Al)$ = 0 ppm) for ^{27}Al, water ($\delta_{iso}(^{1}H)$ = 4.6 ppm) for ^{1}H and adamantane ($\delta_{iso}(^{13}C)$ = 38.48 ppm) for ^{13}C[25]. The magic angle was set by minimizing the line width of the spinning side bands lines from the ^{23}Na resonance in $NaNO_3$. The ^{1}H single pulse experiments recorded on the Bruker 950 MHz spectrometer showed a significant background signal,

which was adjusted for by subtracting a background spectrum. However, this correction made the determination of the relative intensities less precise, hence these are not reported. SSNMR spectra were analyzed using QuadFit[26], MestReNova 6.1.1, TopSpin 2.1, and VnmrJ 4.2

3. Results and discussion

3.1 Bulk composition: PXRD, elemental analysis and IR Spectroscopy

PXRD were recorded of all samples in order to confirm the formation of LDHs and intercalation of PAS. The PXRD diffractograms contain the broad reflections, which is characteristic for LDHs with organic anions intercalated[8, 27-30], as illustrated in Fig. 2. The broad reflections are associated with the low crystallinity of the samples due to a large number of stacking faults[31-33]. Thus, PXRD becomes less useful for such LDHs due to the larger uncertainty of the determined crystallographic parameters. The estimated unit cell parameter are reported in Table 1 and were determined using the (003), (006), and (110) reflections and indexed with a hexagonal unit cell. The inter-layer distance ($c' = c/3$ in Fig. 1) for MgAl-PAS, ZnAl-PAS, and CaAl-PAS are 14.8(3) Å, 15.4(1) Å, and 17.6(1) Å, as determined from the (003) reflection. These values match reasonably with what is expected for PAS intercalated into the structure of LDHs, as the *c'* for nitrate containing MgAl, ZnAl and CaAl LDHs are 8.6 to 8.9 Å in agreement with earlier reported values for PAS incorporated in ZnAl LDHs[10, 34]. The larger interlayer distance for the CaAl-PAS is due to the larger Ca^{2+} ion and slightly different crystal structure, c.f., Fig. 1. From the determined *c´* values it is clear that a large anion such as PAS is incorporated into the LDHs. We note that decarboxylation of PAS to m-aminophenol occurs at ca. 70 °C for the pure compound and that this should be taken into account during synthesis[35, 36]. Thus, hydrothermal treatment cannot be used to improve the crystallinity of the samples[10]. However, both

FTIR (Fig. SI-2) and ^{13}C CP-MAS NMR (Fig.3, vide infra) confirm the presence of PAS. The PXRD diffractogram of ZnAl-PAS contains no crystalline impurities whereas those for MgAl-PAS and CaAl-PAS contain one and three narrow reflections of low intensity, respectively, as illustrated in Fig. 2. These are ascribed to unknown impurities, as they do not match PAS, aluminum oxides or hydroxides impurities such as bayerite, boehmite, and gibbsite, nor the respective divalent metal hydroxides ($M(II)(OH)_2$) [37, 38].

According to the ICP results (Table 1) ZnAl-PAS has a Zn:Al ratio of 2:1, whereas MgAl-PAS and CaAl-PAS contains 2.1(1) % and 7.3(1) % excess Al. This points towards the presence of an amorphous Al phase not detected by PXRD, as recently reported by Pushparaj et al. for ZnAl LDHs with small inorganic anions intercalated[10]. From ICP and PXRD only reflections from the LDH are seen for MgAl-PAS and ZnAl-PAS. CaAl-PAS contains 7.3(1) % excess Al according to ICP, but PXRD shows no reflections, which can be assigned to crystalline Al phases. Thus, to obtain further insight we performed a series of ^{1}H, ^{13}C, and ^{27}Al SSNMR experiments.

3.2 Solid state NMR spectroscopy

3.2.1 ^{13}C CP-MAS spectroscopy

^{13}C CP-MAS and ^{1}H MAS NMR were employed in order to investigate whether PAS did undergo thermal decomposition to m-aminophenol[35, 36]. FTIR point towards the intercalation of PAS (see supporting information SI-2), but it is very difficult to distinguish between the intercalation of the thermal decompositions products of PAS and carbonate (CO_3^{2-}) by FTIR. The ^{13}C CP-MAS NMR spectra of the three LDHs closely resemble that of pure PAS (Fig. 3) although the individual lines are much broader. Moreover, we do observe small changes in isotropic shifts especially for C1, C2 and C5,

which most likely reflects that the spectrum of pure PAS is the acidic form whereas the LDHs contain the anion. The low signal to noise and broad lines reflect variations in the local ^{13}C environments in the interlayer due to e.g. stacking faults and different orientation within the interlayer. Table 2 summarizes the chemical shifts determined and their assignment, which is based on the liquid state ^{13}C NMR spectra of PAS-H. No impurities such as the thermal decomposition product m-aminophenol were observed in the ^{13}C CP-MAS NMR spectra (Fig. 3) except a broad background in the region $\delta(^{13}C) \approx$ 116-127 ppm from the endcap and spacers.

3.2.2 The purity of the LDHs from ^{27}Al SSNMR

^{27}Al single pulse and 3QMAS NMR spectra were recorded both to check the purity of the products in light of a recent study, which revealed larges amount of amorphous Al impurities despite Al contents close to the ideal 33 %, and also to probe the origin of the excess Al in the CaAl LDH sample[10]. Such impurities may cause serious problems especially in relation to the use of LDHs in drug formulation. The ^{27}Al NMR single pulse spectra are seen in Fig. 4 whereas a representative ^{27}Al 3QMAS NMR spectrum is illustrated for MgAl-PAS in Fig. 5. These 3Q MAS spectra were recorded at an ultra-high field (22.3 T) and high field (14.1 T) with the best resolution at 14.1 T due to similar values of isotropic chemical shifts for the different Al sites. Table 3 summarizes the parameters obtained from analysis of both single pulse and 3QMAS NMR spectra at the three magnetic field strengths (11.7, 14.1 and 21.3 T) spectra for each LDH sample. The ^{27}Al 3QMAS NMR spectra at 14.1 and 22.3 T were used to estimate $\delta_{iso}(^{27}Al)$ and the quadrupolar product, $P_Q = C_Q(1+\eta^2/3)^{0.5}$ for the ^{27}Al sites. These values were employed as starting parameters in simulations of the ^{27}Al single pulse NMR spectra at three fields (11.7, 14.1, and 22.3 T). The objective was to obtain a single set of NMR parameters, which in the most optimal way reproduce the spectra at all three fields, and these parameters are presented in Table

3. The simulations employed a Gaussian distribution of both the quadrupole coupling and the asymmetry parameters The LDH site is the dominating resonance, but simulations of the single pulse spectra using a single Al site (LDH) shows a significant residual. Moreover, the ^{27}Al 3QMAS NMR spectra also show the presence of at least one, and possibly two or three other ^{27}Al resonances for MgAl-PAS, ZnAl-PAS, and CaAl-PAS c.f., Table 3. These non-LDH phases, which in total constitute between 20 and 41 % of the total intensities, are considered amorphous for the MgAl-PAS and ZnAl-PAS samples, due to the lack of non-LDH reflections in the PXRD diffractograms (Fig. 2). The observation of excess Al in both MgAl-PAS and ZnAl-PAS points to a lower Al content in the LDH layer. However, due to the broad line width of the (110) reflection this cannot be used to determine the M(II):Al ratio. The M(II):Al ratio in the three LDHs were estimated from the ICP results and the Al impurities quantified by ^{27}Al NMR are used to correct these values. For MgAl-PAS the Mg:Al ratio is between 2:1 and 3:1 (30 (4) % Al), whereas the ratio for the ZnAl-PAS sample is found to be 3:1 (23(4) % Al) within the experimental error. For CaAl-PAS a ratio of 2:1 is obtained (32(1) % Al). Generally, the M(II):Al ratios can vary between 2:1 and 6:1 for MgAl and ZnAl LDHs whereas for CaAl LDHs this is restricted to 2:1.

The LDH site was for all samples found to have a C_Q of 1.6 MHz, which is in excellent agreement with earlier reports values for MgAl-, and ZnAl-LDHs with simple anions intercalated[10, 12]. For CaAl LDHs does the C_Q match the low-temperature form of the structurally related CaAl-LDH with chloride intercalated (Friedel's salt)[39]. This reflects that the local environment in the cation layer of LDHs is nearly independent of the anion intercalated and that SSNMR can be used to fingerprint LDHs. A recent study of two benzoxaborolates into MgAl LDHs by ion-exchange into a MgAl LDH reported only one Al site[18], but did not report any SSNMR parameters. It should be emphasized that neither

PXRD nor elemental analysis for MgAl-PAS and ZnAl-PAS suggest the presence of fairly large concentrations of impurities.

3.2.2 Local environments in MgAl-, ZnAl- and CaAl-PAS from ^{1}H MAS and ^{1}H DQ MAS NMR as well as ^{27}Al{^{1}H} HETCOR spectra

To gain insight into the local proton environments in the three samples and thereby further information about the M(II):Al ratios, ^{1}H MAS NMR spectra were recorded at 950 MHz. Moreover, a partially deuterated MgAl sample (MgAl-D_2O) was studied and this showed an increased resolution especially in the 2D SSNMR spectra, as reported earlier[40].

The 1D ^{1}H spectra (Fig. 6) were analyzed by deconvolution, from which the isotropic shifts and relative intensities were obtained and assigned using ^{27}Al{^{1}H} HETCOR spectra and the ^{1}H{^{1}H} DQ (Figs. 7,8 SI-3, and SI-5). We will in the following first focus on MgAl-PAS and ZnAl-PAS, which are isostructural, followed by a CaAl-LDH. High-resolution ^{1}H MAS NMR spectra have been reported for MgAl- and ZnAl LDHs and the different resonances are assigned[10, 11]. High-resolution ^{1}H MAS NMR spectra of CaAl-LDHs have not been reported to our knowledge. Two ^{1}H resonances are expected for an LDH with a 2:1 M(II):Al ratio, one resonance from the $M(II)_2$Al-OH group and one from the interlayer water [11, 14]. The most intense resonance in the ^{1}H spectra is observed at 4.1-4.4 ppm (Fig. 6) and is assigned to interlayer water in agreement with earlier studies[10, 11, 14]. The intense water resonance reflects large water content in the intergallery. In line with these studies, the ^{1}H resonances with $\delta_{iso}(^{1}H)$ = 3.1(4) and 3.0(6) ppm are assigned to Mg_2Al-OH and Zn_2Al-OH, respectively. Moreover, this is confirmed by ^{27}Al{^{1}H}-HETCOR NMR spectra (Figs. 7b and SI-5b). A less intense resonance at $\delta_{iso}(^{1}H) \approx$ 1.0-1.1 ppm is observed for MgAl-PAS and ZnAl-PAS c.f. Table 4, which from ^{1}H DQ MAS

NMR spectra clearly is seen to be connected to both the Mg_2Al-OH (Zn_2Al-OH) and interlayer water for MgAl-PAS (ZnAl-PAS) indicating that this is part of the cation layer in the LDH. Thus, we assign this to Mg_3-OH (Zn_3-OH) groups in agreement with a M(II):Al ratio above 2:1 c.f. Sec. 3.2.1. For Mg_3-OH, the $\delta_{iso}(^1H)$ values agree well with earlier reported data[11, 13]. The ^1H single pulse spectra of all three samples contain two sites with $\delta_{iso}(^1H)$ = 5.6 and 7.2 ppm with a relative intensity of approximately 2:1. ^1H DQ MAS NMR spectra (Figs. 7a, 8a, and SI-5a) show that these resonance are in close proximity, and not correlated with ^{27}Al according to $^{27}Al\{^1H\}$ HETCOR NMR spectra (Figs. 6b and SI-5b). Hence we assign these to the three aromatic protons H3, H5 and H6 of which two have similar chemical shifts. This is most likely H3 and H5 based on the ^1H liquid state NMR spectra. The absence of cross-peaks between the aromatic protons in PAS and the LDH cation shows that these are not in close proximity, in agreement with the expected orientation of PAS in the interlayer (Fig. 1). The ^1H MAS NMR spectrum of CaAl-PAS in Fig. 7c is more complex and contains two intense peaks with $\delta_{iso}(^1H)$ = 1.3 and 2.9 ppm, respectively in addition to the interlayer water (4.2 (5) ppm) c.f. Table 4. These three resonances are in close proximity according to ^1H DQ MAS NMR spectra (Fig. 8a) and are therefore part of the cation layer in the LDH. Moreover, the $^{27}Al\{^1H\}$-HETCOR spectrum in Fig. 8b shows an intense cross-peak for the site with $\delta_{iso}(^1H)$ = 1.3 ppm to the ^{27}Al NMR resonance from the LDH. Thus, we assign this to the Ca_2Al-OH group whereas the site with $\delta_{iso}(^1H)$ = 2.9 ppm is assigned to the water molecular directly coordinated to Ca (Fig. 1c). Also for CaAl-PAS, are no correlations between the aromatic protons and the –OH groups seen.

4. Conclusions

The intercalation of PAS in MgAl, ZnAl, and CaAl LDHs was investigated in detail using multi-nuclear SSNMR experiments in combination with PXRD, IR, and elemental analysis and illustrates that SSNMR provides information which is difficult to obtain from other characterization techniques. ^{13}C CP-MAS NMR confirmed intercalation of the drug and that no degradation of this had happened during synthesis. ^{27}Al SSNMR show fairly large amount of amorphous impurities in all samples, which were not detected by PXRD and not directly evident from elemental analysis (ICP) except for CaAl-PAS, which contained excess Al. In addition, the actual M(II):Al(III) ratio in the LDH-PAS phases was determined by combining ^{1}H and ^{27}Al NMR data with elemental analysis. This showed a lower Al content than predicted by ICP, i.e., "hidden Al amorphous impurities". MgAl and ZnAl contained 30 and 24 % Al in the LDH phase in contrast to the 33 % Al in the reactant mixture. CaAl-PAS had the expected 2:1 ratio, but did contain Al impurities, as also observed by elemental analysis. The ^{27}Al quadrupole coupling from the single LDH site was for all samples found 1.6 MHz, which is agreement with earlier reported values[10, 12]. The δ_{iso}(^{27}Al) values show little variation upon modification of the anion, but do change with the choice of M(II) ion. Moreover, we reported the first high resolution ^{1}H MAS NMR spectrum for a CaAl LDH and the resonances were assigned using ^{1}H DQ MAS NMR and ^{27}A{^{1}H}-HETCOR SSNMR experiments. Thus, our work demonstrates that SSNMR is an excellent experimental technique for characterization of LDHs with drugs intercalated and provides a unique insight into the atomic level structure of LDHs.

5. Acknowledgements:

The authors are gratefully for financial support from the Villum Foundation via the "Villum Young Investigator Program" grant VKR022364 (UGN, NDJ, and SSNMR equipment) and 600 MHz NMR (Villum Center for Bioanalytical Services, 600 MHz NMR instrument). Access to the 950 MHz

NMR spectrometer at the Danish Center for Ultrahigh-Field NMR Spectroscopy (Ministry of Higher Education and Science grant AU-2010-612-181) is acknowledged. Ms. Carina K. Lohmann (Biology Institute, University of Southern Denmark) is acknowledged for the ICP analysis.

Tables

Table 1: Unit cell parameter determined from the PXRD diffractograms in Fig. 2 indexed using a hexagonal unit cell and the total Al content determined from ICP.

Sample	**a(Å)**	**c(Å)**	**Al (%)**
MgAl-PAS	3.0(1)	47.7(9)	35.4(1)
ZnAl-PAS	3.0(1)	47.3(2)	33.2(1)
CaAl-PAS	3.3(1)	50.6(3)	40.6(1)

Table 2: $\delta_{iso}(^{13}C)$ obtained from analysis of ^{13}C CP MAS data recorded at 11.7 T (see Fig. 3).

Sample / Assignment	**MgAl-PAS (ppm)**	**ZnAl-PAS (ppm)**	**CaAl-PAS (ppm)**	**Pure PAS-H (ppm)**
C1	176(1)	175(1)	176(2)	176(1)
C2/4	98(3)	98(1)	100(3)	99(1)
C3	166(3)	166(1)	166(3)	163(1)
C2/4	102(2)	102(2)	102(3)	99(1)
C5	106(3)	106(2)	106(4)	108(1)
C6	133(2)	133(3)	133(3)	135(1)
C7	154(1)	154(2)	153(3)	155(1)

Table 3: ^{27}Al NMR parameters obtained, which provide an overall best fit of the ^{27}Al SSNMR spectra obtained at three field strengths (11.7, 14.1, and 22.3 T) as shown in Figs. 4, 5, and SI-4.

Sample	**Assignment**	**δ_{iso}(^{27}Al) (ppm)**	**C_Q (MHz)**	**η**	**I(%)**
MgAl-PAS	LDH	11.2(4)	1.6(2)	0.0(1)	80(6)
		9.2(8)	3.3(3)	0.2(2)	20(5)
ZnAl-PAS	LDH	15.5(5)	1.6(2)	0.0(1)	59(5)
		13.1(4)	2.9(3)	0.5(2)	10(4)
		11.0(6)	4.0(4)	0.5(3)	31(7)
CaAl-PAS		14.8(8)	2.0(2)	0.5(2)	5(4)
	LDH	11.0(2)	1.6(1)	0.0(1)	65(4)
		8.5(3)	2.5(3)	0.2(3)	5(2)
		8.0(8)	4.5(4)	0.2(3)	25(3)

Table 4: ^{1}H parameter obtained from deconvolutions of ^{1}H spectra obtained at 22.3 T and assigned using the ^{1}H DQ MAS NMR and $^{27}Al\{^{1}H\}$ HETCOR NMR experiments.

Sample	**Assignment**	**$\delta_{iso}(^{1}H)$ (ppm)**
MgAl-PAS	Mg_3OH	1.1(7)
	Mg_2AlOH	3.1(5)
	Water	4.3(5)
	PAS	5.7(2)
	PAS	7.2 (3)
ZnAl-PAS	Zn_3OH	1.0(5)
	Zn_2AlOH	3.0(7)
	Water	4.2(4)
	PAS	5.8(6)
	PAS	7.2(7)
CaAl-PAS	Ca_2AlOH	1.3(5)
		2.3(3)
	$Ca\text{-}H_2O$	2.9(6)
	Water	4.2(4)
	PAS	5.6(7)
	PAS	7.3(7)

Figures:

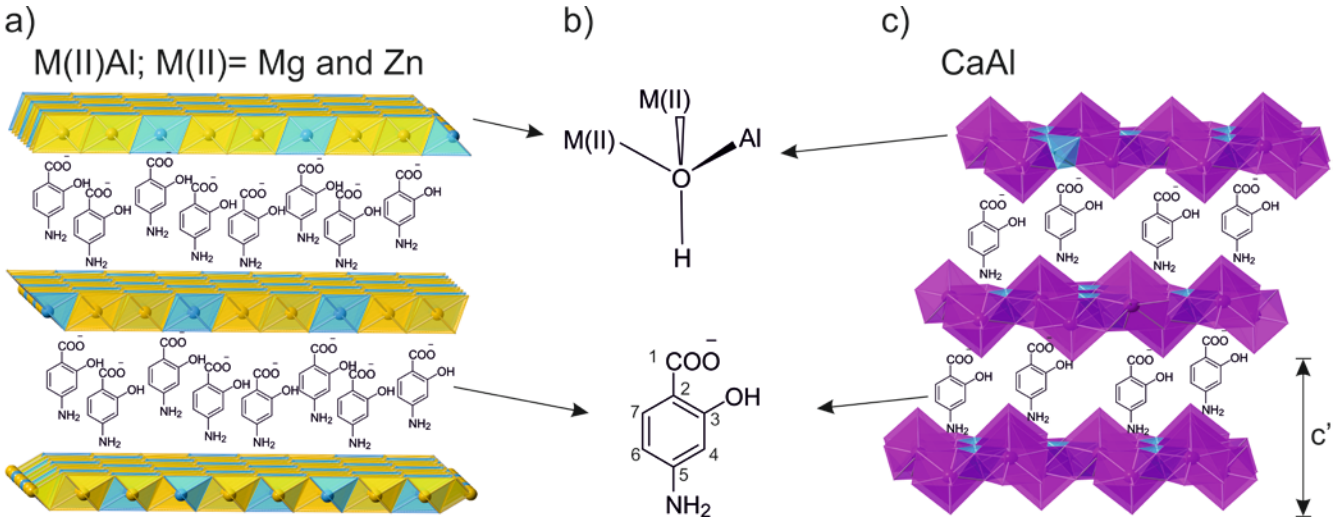

Fig. 1: a) The $M(II)_2Al(OH)_6$ LDH structure, which contain octahedrally coordinated cations and c) The $Ca_2Al(OH)_6$ LDH structure where the Ca (II) ions are hepta coordinataed (six OH and one water ligand) and Al(III) is octahedrally coordinated (six OH groups). b) The single -OH group in a cation ordered LDH with a M(II):M(III) ratio of 2:1 is $M(II)_2Al$-OH. The structure of PAS with the individual C atoms labeled. We note that for samples with a Al content below 33.3 % $M(II)_3$-OH groups are expected[11, 41, 42].

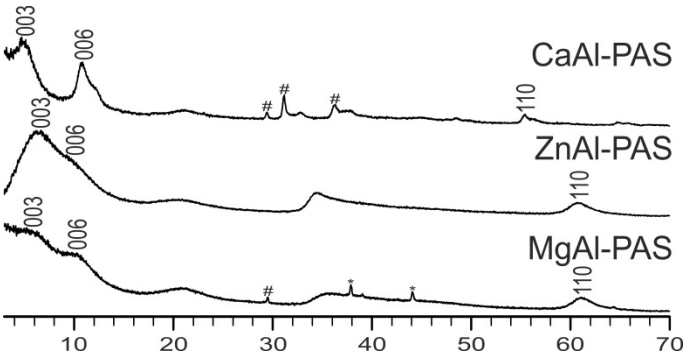

Fig. 2: PXRD diffractograms of the three LDH samples with characteristic LDH reflections assigned. # marks unknown impurities and * are reflections from the sample holder.

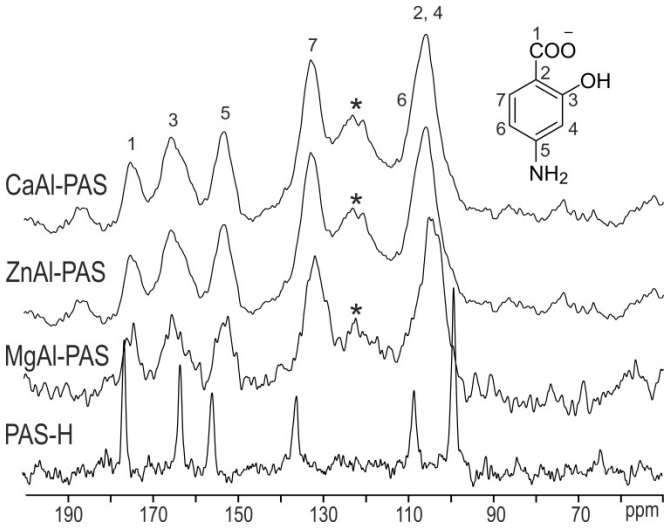

Fig. 3: ^{13}C CP MAS SSNMR spectra of the three LDHs and pure PAS-H recorded at 11.7 T using 12 kHz spinning speed. The LDHs contain PAS, whereas the reference spectrum is of the acidic form (PAS-H). An asterisk (*) marks the ^{13}C resonance from the rotor background.

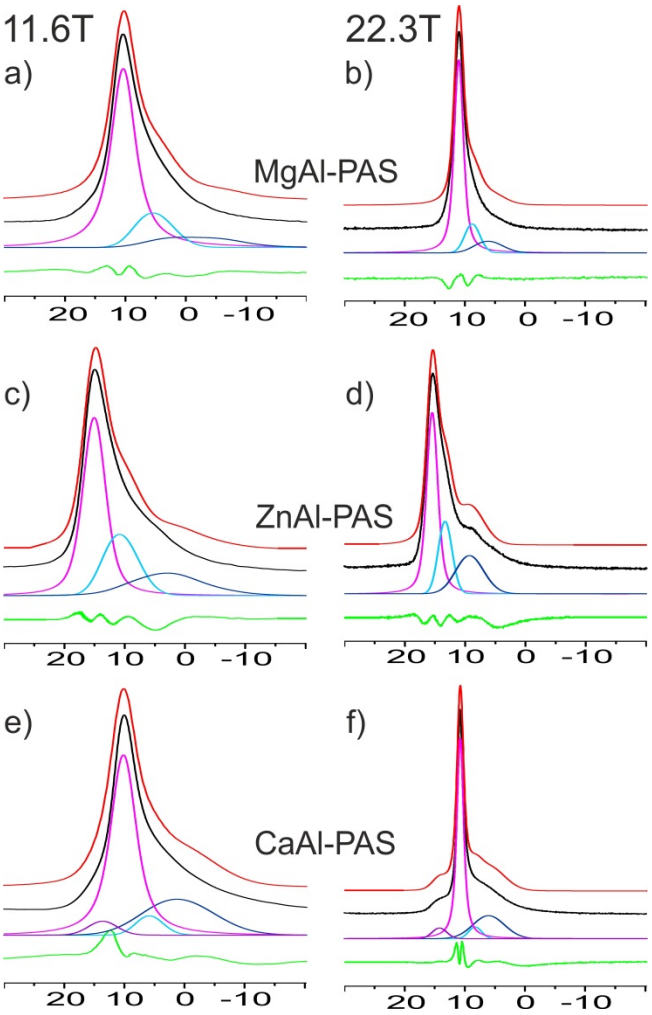

Fig. 4: Experimental (black) and simulated ^{27}Al MAS NMR spectra (red) at 11.6 T for a) MgAl-PAS) c) ZnAl-PAS, and e) CaAl-PAS whereas the corresponding 22.3 T spectra are shown in b) MgAl-PAS d) ZnAl-PAS, and f) CaAl-PAS, respectively. Two to four Al sites (shown as purple, blue and light blue) were used in the deconvolution, one from the LDH resonance and the others from amorphous Al impurities c.f., Table 3. The green spectra show the differences between experimental and simulated spectra.

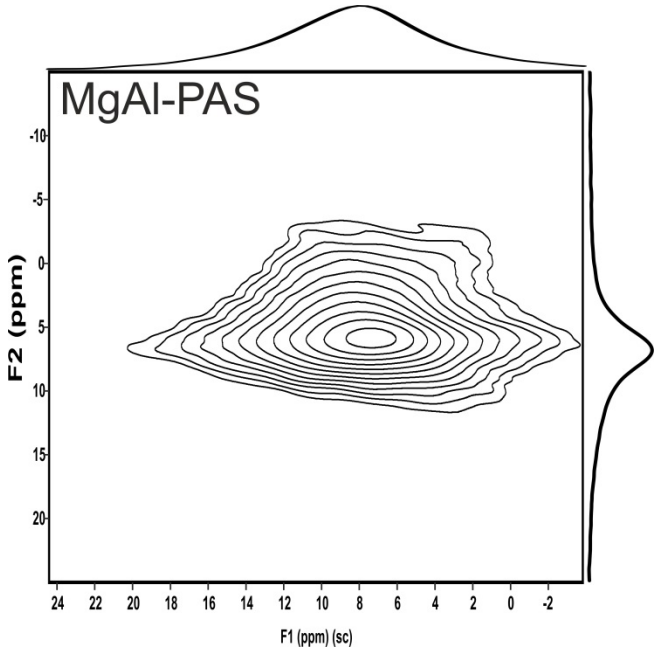

Fig. 5: ^{27}Al 3QMAS NMR spectrum of MgAl-PAS, recorded at 14.1 T using 15 kHz spinning.

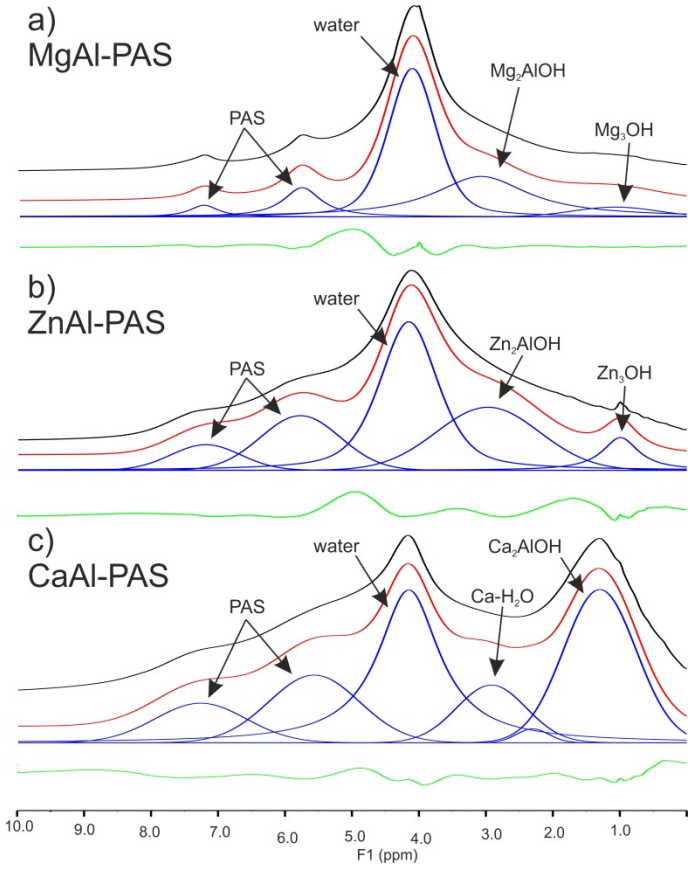

Fig. 6: Experimental (black) and simulated (red) ^{1}H MAS NMR spectra of a) MgAl-PAS, b) ZnAl-PAS, c) CaAl-PAS recorded at 22.3 T (35 kHz spinning). Simulations of the individual sites (blue) and the difference (green) between experimental and simulated spectra are also shown. The resonances were assigned using the ^{1}H DQ MAS NMR spectra in Fig. 7, 8, and SI-5 in combination with earlier reported values for ZnAl and MgAl LDHs[10, 11].

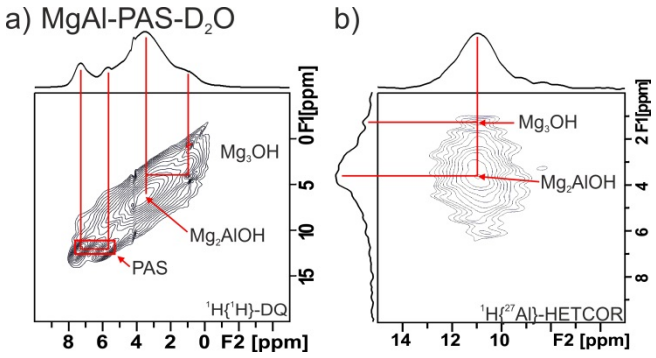

Fig. 7: a) ^{1}H DQ MAS NMR spectrum of MgAl-D_2O LDH with the individual cross-peaks assigned and b) ^{27}Al{^{1}H}-HETCOR NMR spectrum for the same sample.

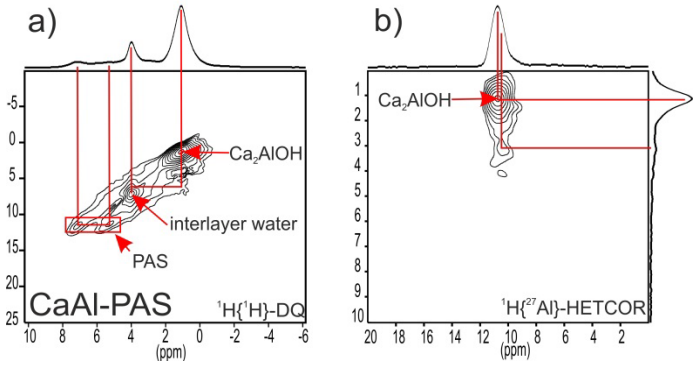

Fig. 8: a) ^{1}H DQ MAS NMR spectrum of CaAl-PAS LDH with the individual cross-peaks assigned and b) ^{27}Al {^{1}H}-HETCOR spectrum.

7. **References**

1. Bi, X.; Zhang, H.; Dou, L., Layered Double Hydroxide-Based Nanocarriers for Drug Delivery. *Pharmaceutics* **2014,** *6*, (2), 298-332.
2. Goh, K. H.; Lim, T. T.; Dong, Z., Application of layered double hydroxides for removal of oxyanions: a review. *Water Res* **2008,** *42*, (6-7), 1343-68.
3. Vaccari, A., Clays and catalysis: a promising future. *Applied Clay Science* **1999,** *14*, (4), 161-198.
4. Forano, C.; Hibino, T.; Leroux, F.; Taviot-Guého, C., Layered Double Hydroxides. *Developments in Clay Science* **2006,** *1*, 1021-1092.
5. Shao, M.; Zhang, R.; Li, Z.; Wei, M.; Evans, D. G.; Duan, X., Layered Double Hydroxides toward Electrochemical Energy Storage and Conversion: Design, Synthesis and Applications. *Chemical Communications* **2015,** *51*, (88), 15880-15893.
6. Evans, D. G.; Slade, R. C. T., *Structural Aspects of Layered Double Hydroxides*. Springer-Verlag Berlin Heidelberg: 2005.
7. Ambrogi, V.; Fardella, G.; Grandolini, G.; Perioli, L., Intercalation Compounds of Hydrotalcite-Like Anionic Clays with Antiinflammatory Agents — I. Intercalation and In Vitro Release of Ibuprofen. *International Journal of Pharmaceutics* **2001,** *220*, (1–2), 23-32.
8. del Arco, M.; Gutiérrez, S.; Martín, C.; Rives, V.; Rocha, J., Synthesis and Characterization of Layered Double Hydroxides (LDH) Intercalated with Non-Steroidal Anti-Inflammatory Drugs (NSAID). *Journal of Solid State Chemistry* **2004,** *177*, (11), 3954-3962.

9. Del Hoyo, C., Layered Double Hydroxides and Human Health: An Overview. *Applied Clay Science* **2007,** *36*, (1–3), 103-121.

10. Pushparaj, S. S. C.; Forano, C.; Prevot, V.; Lipton, A. S.; Rees, G. J.; Hanna, J. V.; Nielsen, U. G., How the Method of Synthesis Governs the Local and Global Structure of Zinc Aluminum Layered Double Hydroxides. *The Journal of Physical Chemistry C* **2015,** *119*, (49), 27695-27707.

11. Sideris, P. J.; Nielsen, U. G.; Gan, Z.; Grey, C. P., Mg/Al Ordering in Layered Double Hydroxides Revealed by Multinuclear NMR Spectroscopy. *Science* **2008,** *321*, (5885), 113-117.

12. Sideris, P. J.; Blanc, F.; Gan, Z.; Grey, C. P., Identification of Cation Clustering in Mg–Al Layered Double Hydroxides Using Multinuclear Solid State Nuclear Magnetic Resonance Spectroscopy. *Chemistry of Materials* **2012,** *24*, (13), 2449-2461.

13. Cadars, S.; Layrac, G. R.; Gérardin, C.; Deschamps, M. l.; Yates, J. R.; Tichit, D.; Massiot, D., Identification and Quantification of Defects in the Cation Ordering in Mg/Al Layered Double Hydroxides. *Chemistry of Materials* **2011,** *23*, (11), 2821-2831.

14. Petersen, L. B.; Lipton, A. S.; Zorin, V.; Nielsen, U. G., Local Environment and Composition of Magnesium Gallium Layered Double Hydroxides Determined from Solid-State ^{1}H and ^{71}Ga NMR Spectroscopy. *Journal of Solid State Chemistry* **2014,** *219*, 242-246.

15. Reinholdt, M. X.; Babu, P. K.; Kirkpatrick, R. J., Proton Dynamics in Layered Double Hydroxides: A 1H T1 Relaxation and Line Width Investigation. *Journal of Physical Chemistry C* **2009,** *113*, (24), 10623-0631.

16. Reinholdt, M. X.; Babu, P. K.; Kirkpatrick, R. J., Preferential Adsorption of Lower-Charge Glutamate Ions on Layered Double Hydroxides An NMR Investigation. *Journal of Physical Chemistry C* **2009,** *113*, (9), 3378-3381.

17. Hou, X.; Kirkpatrick, R. J., Interlayer Structure and Dynamics of ClO_4-Layered Double Hydroxides. *Chemistry of Materials* **2002,** *14*, 1195-1200.

18. Sene, S.; Bégu, S.; Gervais, C.; Renaudin, G.; Mesbah, A.; Smith, M. E.; Mutin, P. H.; van der Lee, A.; Nedelec, J.-M.; Bonhomme, C.; Laurencin, D., Intercalation of Benzoxaborolate Anions in Layered Double Hydroxides: Toward Hybrid Formulations for Benzoxaborole Drugs. *Chemistry of Materials* **2015,** *27*, (4), 1242-1254.

19. M. Silion (Frunza); D. Hritcu R.; Popa, M. I., Intercalation of Salicylic Acid into ZnAl Layered Double Hydroxides by Ion-Exchange and Coprecipitation Method. *Journal of Optoelectronics and Advanced Materials* **2009,** *11*, (4), 528-534.

20. Min Wei, M. P., Guo, J.; Han, J.; Li,F.: He, J.: Evans, D.G., Duan, X.; Intercalation of L-Dopa into Layered Double Hydroxides: Enhancement of Both Chemical and Stereochemical Stabilities of a Drug through Host-Guest Interactions. *Chemistry of Materials* **2008,** *20*, 5169-5180.

21. Mohanambe, L.; Vasudevan, S., Anionic Clays Containing Anti-Inflammatory Drug Molecules: Comparison of Molecular Dynamics Simulation and Measurements. *Journal of Physical Chemistry B* **2005,** *109*, 15651-15658.

22. Amoureux, J. P.; Fernandez, C., Triple, quintuple and higher order multiple quantum MAS NMR of quadrupolar nuclei. *Solid State Nuclear Magnetic Resonance* **1998,** *10*, 211-223.

23. Geen, H.; Titman, J. J.; Gottwald, J.; Spiess, H. W., Solid-state proton multiple-quantum NMR spectroscopy with fast magic angle spinning. *Chemical Physics Letters* **1994,** *227*, (1), 79-86.

24. Schnell, I.; Watts, A.; Spiess, H. W., Double-Quantum Double-Quantum MAS Exchange NMR Spectroscopy: Dipolar-Coupled Spin Pairs as Probes for Slow Molecular Dynamics. *Journal of Magnetic Resonance* **2001,** *149*, (1), 90-102.

25. Morcombe, C. R.; Zilm, K. W., Chemical shift referencing in MAS solid state NMR. *Journal of Magnetic Resonance* **2003,** *162*, (2), 479-486.

26. Kemp, T. F.; Smith, M. E., QuadFit--A New Cross-Platform Computer Program for Simulation of NMR Line Shapes from Solids with Distributions of Interaction Parameters. *Solid State Nuclear Magnetic Resonance* **2009,** *35*, (4), 243-52.

27. Saifullah, B.; Hussein, M. Z.; Hussein-Al-Ali, S. H.; Arulselvan, P.; Fakurazi, S., Antituberculosis Nanodelivery System with Controlled-Release Properties Based on Para-Amino Salicylate-Zinc Aluminum-Layered Double-Hydroxide Nanocomposites. *Drug design, Development and Therapy* **2013,** *7*, 1365-75.

28. Saifullah, B.; El Zowalaty, M. E.; Arulselvan, P.; Fakurazi, S.; Webster, T. J.; Geilich, B. M.; Hussein, M. Z., Antimycobacterial, Antimicrobial, and Biocompatibility Properties of Para-Aminosalicylic Acid with Zinc Layered Hydroxide and Zn/Al Layered Double Hydroxide Nanocomposites. *Drug design, Development and Therapy* **2014,** *8*, 1029-36.

29. Kang Zou, H. Z., Xue Duan, Studies on the Formation of 5-Aminosalicylate Intercalated Zn–Al Layered Double Hydroxides as a Function of Zn/Al Molar Ratios and Synthesis Routes. *Chemical Engineering Science 6* **2007,** *62*, 2022-2031.

30. Silion, M. F.; Hritcu, D.; Popa, M. I., Intercalation of Salicylic Acid into ZnAl Layered Double Hydroxides by Ionic-Exchange Method. *Optoelectronics and Advanced Materials - Rapid Communications* **2009,** *3*, 817-820

31. Bellotto, M.; Rebours, B.; Clause, O.; Lynch, J.; Bazin, D.; Elkaïm, E., A Reexamination of Hydrotalcite Crystal Chemistry. *Journal of Physical Chemistry* **1996,** *100*, 8527-8534.

32. Radha, A. V.; Kamath, P. V.; Shivakumara, C., Conservation of Order, Disorder, and "Crystallinity" during Anion-Exchange Reactions among Layered Double Hydroxides (LDHs) of Zn with Al. *The Journal of Physical Chemistry B*, **2007**; 111, 3411-3418.

33. Roussel, H.; Briois, V.; Elkaim, E.; de Roy, A.; Besse, J. P., Cationic Order and Structure of [Zn−Cr−Cl] and [Cu−Cr−Cl] Layered Double Hydroxides: A XRD and EXAFS Study. *The Journal of Physical Chemistry B*, **2000**; 104, 5915-5923.

34. Wang, S.-L.; Liu, C. H.; Wang, M. K.; Chuang, Y. H.; Chiang, P. N., Arsenate Adsorption by Mg/Al–NO3 Layered Double Hydroxides with Varying the Mg/Al ratio. *Applied Clay Science* **2009,** *43*, 79-85.

35. Vetuschi, C.; Ragno, G.; Mazzeo, P., Determination of P-Aminosalicylic Acid and m-Aminophenol by Derivative UV-Spectrophotometry. *Journal of Pharmaceutical & Biomedical Analysis* **1988,** *6*, 383-391.

36. Wesolowski, M., The Decarboxylation and Thermal Stability of P-Amino-Salicylic Acid and its Salts. *Thermochimica Acta* **1977,** *21*, (2), 243-253.

37. Christoph, G. G.; Corbató, C. E.; Hofmann, D. A.; Tettenhorst, R. T., The Crystal Structure of Boehmite. *Clays and Clay Minerals* **1979,** *27*, (2), 81-86.

38. Damodaran, K.; Rajamohanan, P. R.; Chakrabarty, D.; Racherla, U. S.; Manohar, V.; Fernandez, C.; Amoureux, J.-P.; Ganapathy, S., Triple-Quantum Magic Angle Spinning ^{27}Al NMR of Aluminum Hydroxides. *Journal of the American Chemical Society* **2002,** *124*, (13), 3200–3201.

39. Andersen, M. D.; Jakobsen, H. J.; Skibsted, J., Characterization of the alpha-beta Phase Transition in Friedels Salt ($Ca_2Al(OH)_6Cl\cdot_2H_2O$) by Variable-Temperature ^{27}Al MAS NMR Spectroscopy. *Journal of Physical Chemistry A* **2002,** *106*, 6676-6682.

40. Yu, G.; Shen, M.; Wang, M.; Shen, L.; Dong, W.; Tang, S.; Zhao, L.; Qi, Z.; Xue, N.; Guo, X.; Ding, W.; Hu, B.; Peng, L., Probing Local Structure of Layered Double Hydroxides with ^{1}H Solid-State NMR Spectroscopy on Deuterated Samples. *The Journal of Physical Chemistry Letters* **2014,** *5*, (2), 363-369.

41. Allmann, R.; Jepsen, H. P., Die Struktur des Hydrotalkits. *Neues Jahrbuch fuer Mineralogie* **1969**, 544-551.

42. Rousselot, I.; Taviot-Guého, C.; Leroux, F.; Léone, P.; Palvadeau, P.; Besse, J.-P., Insights on the Structural Chemistry of Hydrocalumite and Hydrotalcite-like Materials: Investigation of the Series $Ca_2M^{3+}(OH)_6Cl{\cdot}2H_2O$ (M^{3+}: Al^{3+}, Ga^{3+}, Fe^{3+}, and Sc^{3+}) by X-Ray Powder Diffraction. *Journal of Solid State Chemistry* **2002,** *167*, (1), 137-144.

Supporting Information

A solid state NMR study of layered double hydroxides intercalated with para-amino salicylate, a tuberculosis drug

Nicholai Daugaard Jensen[1], Morten Bjerring[2], and Ulla Gro Nielsen[1,*]

Department of Physics, Chemistry, and Pharmacy, University of Southern Denmark, Campusvej 55, 5230 Odense M, Denmark

[2] Department of Chemistry and Interdisciplinary Nanoscience Center (iNANO), University of Aarhus, Gustav Wiedsvej 14, 8000 Aarhus C, Denmark

*corresponding author: email ugn@sdu.dk phone + 456550 4401

Table of contents

SI-1: Syntheses Parameters

Table SI-1: Parameters used for the syntheses of the three LDH samples

	m $(M(II)(NO_3)_2$	**m $Al(NO_3)_3$**	**m PAS-H**	**Synthesis pH**	**Ageing time**
MgAl-PAS	1.9828 g	1.2507 g	0.7660 g	10.0(3)	18 h
ZnAl-PAS	1.9848 g	1.2512 g	0.7668 g	8.5(5)	15 h
CaAl-PAS	1.5778 g	1.2516 g	0.7676 g	12.0(1)	24 h

SI-2: FT-IR

FT-IR were recorded to study the LDH's structure and especially the incorporated anions. All samples exhibit the characteristic $\delta(H_2O)$ and ν(O-H) band, which originate from interlayer water and the LDHs, respectively (Figure SI-2). Moreover, the ν(C-C), δ(O-H), and δ(C-H) vibrations as well as the $\nu_{as}(COO^-)$ and $\nu_s(COO^-)$ vibrations, which can be assigned to PAS are also observed. The latter two show that PAS is deprotonated[1], which points towards PAS being intercalated in the LDHs structure. It should be noted that the ν_s vibrations can be difficult to distinguish from the ν_3 vibrations from CO_3.[2] Furthermore, a band at 1384 cm^{-1} is observed in all samples, which fit with the $\nu_3(NO_3)$[2] for nitrate. This suggests small amounts of nitrate impurities, which is in contrast to the results from PXRD, where no sign of the nitrate ion is seen.

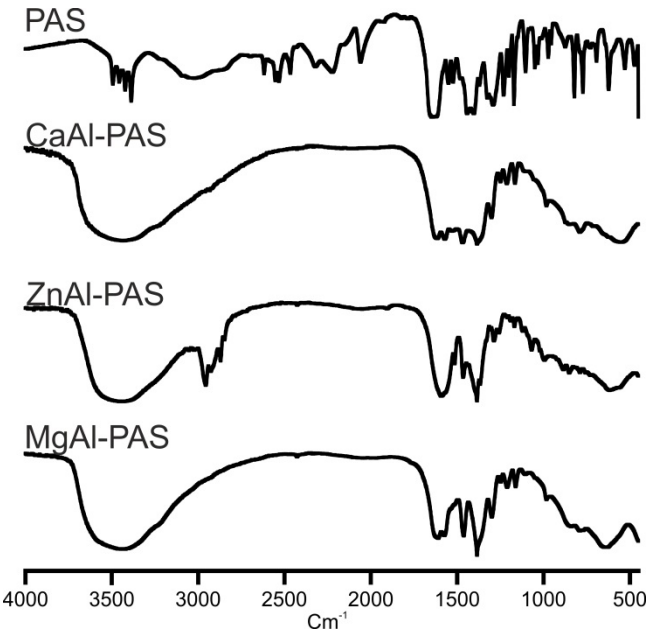

Fig. SI-2: FT-IR spectra of the three LDH samples and PAS. The assignment of the vibrations is given in Table SI-2.

Table SI-2: Characteristic vibration in cm^{-1} observed in FTIR spectra assigned using earlier data for LDHs and PAS[1-2].

Assignment	**MgAl (cm^{-1})**	**ZnAl (cm^{-1})**	**CaAl (cm^{-1})**	**Free PAS (cm^{1})**
ν(O-H)	3445	3435	3441	-
ν(COOH)	-	-	-	1641
ν(C-C)	1527, 1461	1513, 1465	1522, 1468	1523, 1448
δ(O-H)	1299, 1161	1286, 1168	1301, 1164	1294, 1381
δ(C-H)	1106	1090	1103	1112
	982	993	982	971
$\nu_{as}(COO^-)$	1572	1560	1571	-
$\nu_{s}(COO^-)$	1363	1368	1366	-
$\nu_{3}(NO_3)$	1384	1385	1384	-
$\delta(H_2O)$	1608	1592	1613	-

SI-3: 2D SSNMR spectra of ZnAl-PAS

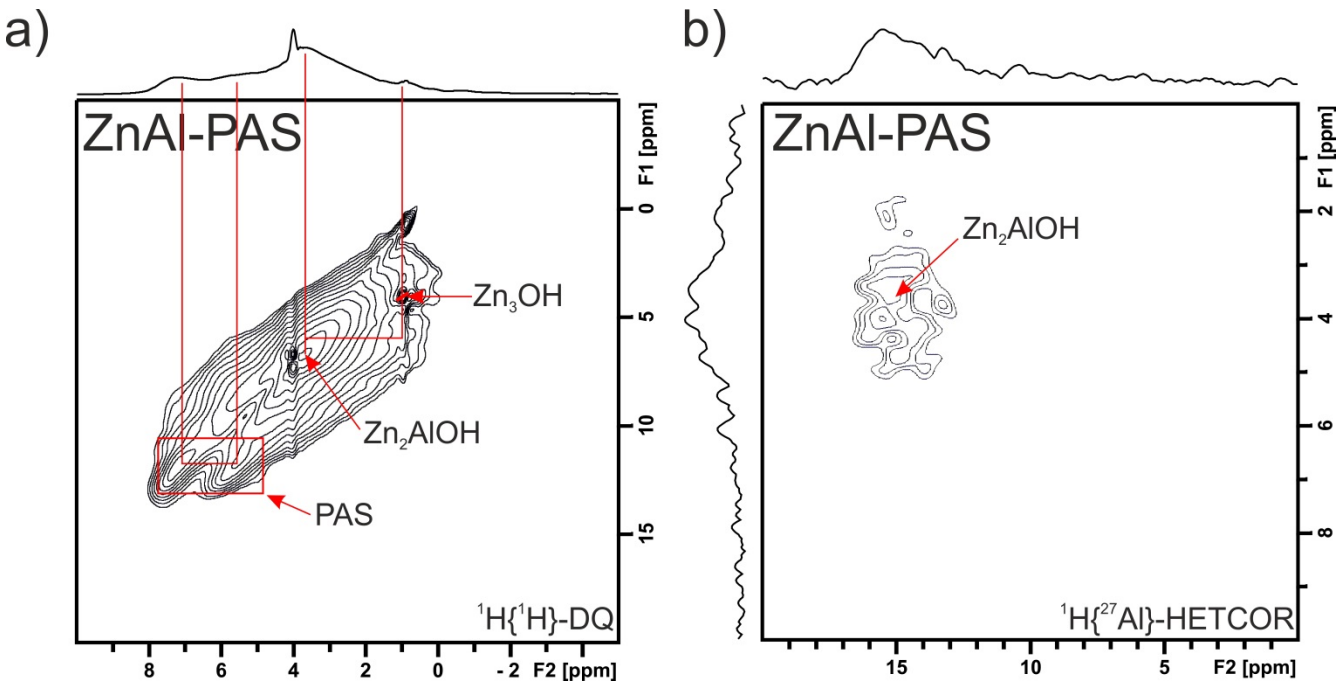

Figure SI-3: a) ^{1}H DQ MAS NMR DQ and b) ^{27}Al{^{1}H} HETCOR NMR spectra of ZnAl-PAS recorded at 950 MHz.

SI-4: ^{27}Al 3QMAS NMR Spectra at 14.1 T

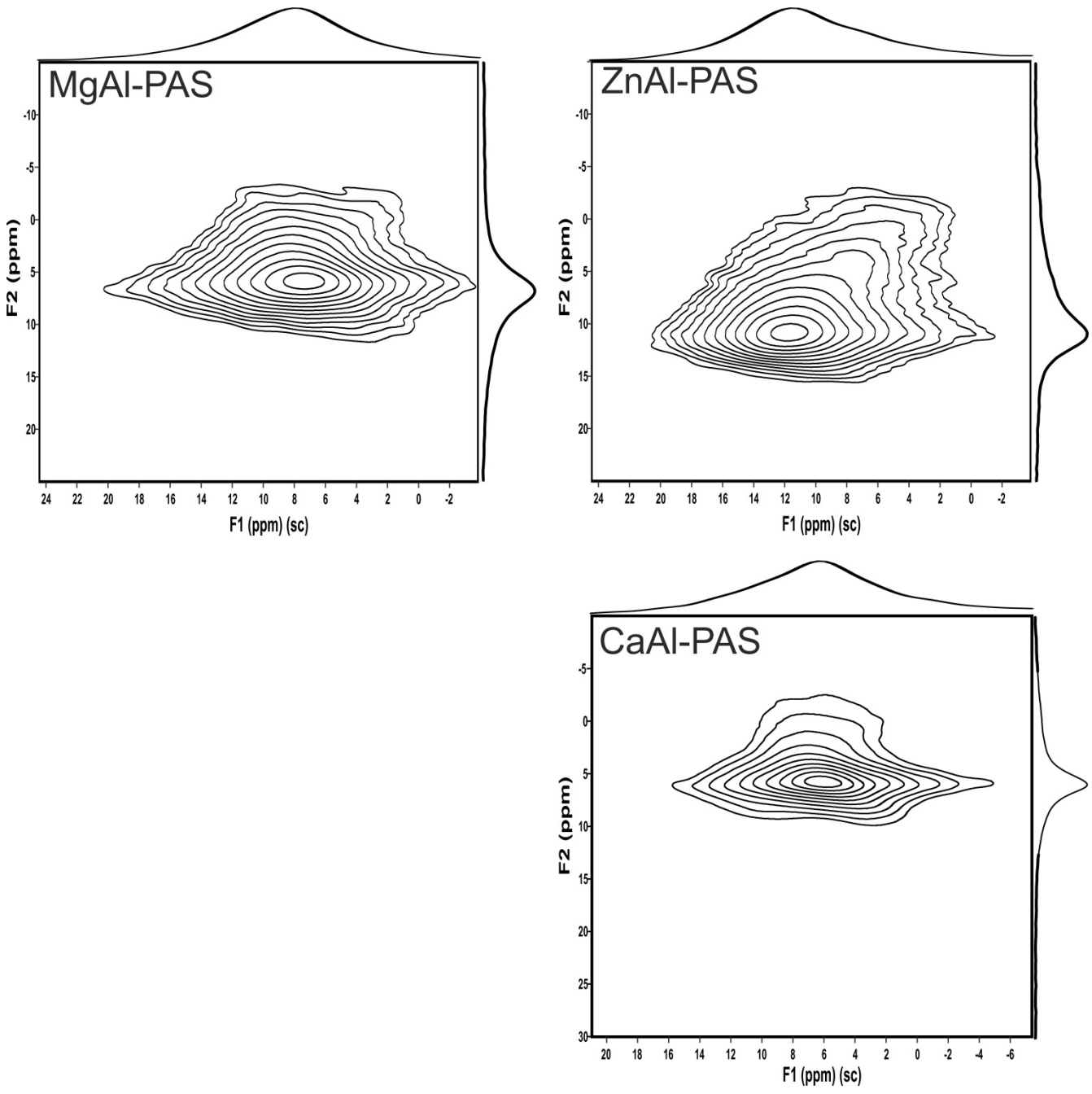

SI-4: ^{27}Al 3QMAS NMR spectra of the MgAl-, ZnAl-, and CaAl-PAS recorded at 14.1 T using 15 kHz spinning.

SI-5: 2D SSNMR spectra of MgAl-PAS

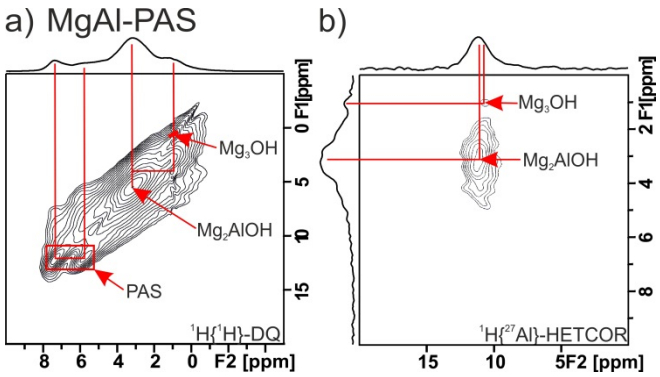

SI-5: a) ^{1}H DQ MAS NMR and b) ^{27}Al{^{1}H}-HETCOR spectra of MgAl-PAS LDH with the individual cross-peaks assigned and recorded at 950 MHz.

References

1. Saifullah, B.; Hussein, M. Z.; Hussein-Al-Ali, S. H.; Arulselvan, P.; Fakurazi, S., Antituberculosis Nanodelivery System with Controlled-Release Properties Based on Para-Amino Salicylate-Zinc Aluminum-Layered Double-Hydroxide Nanocomposites. *Drug Design, Development and Therapy* **2013**, *7*, 1365-75.

2. Goh, K. H.; Lim, T. T.; Dong, Z., Application of Layered Double Hydroxides for Removal of Oxyanions: A Review. *Water Research* **2008**, *42*, 1343-68.